Molecular Crystals and Liquid Crystals
Publication details, including instructions for authors and subscription information:
http://www.tandfonline.com/loi/gmcl20

Anti-Stokes Raman Scattering and Luminescence in Carbon Nanotube Nanostructures

S. Lefrant [a], J. P. Buisson [a], J. Y. Mevellec [a], F. Massuyeau [a], J. Wery [a], M. Baibarac [b] & I. Baltog [b]

[a] Institut des Matériaux Jean Rouxel, 2 rue de la Houssinière, B.P.32229, 44322, Nantes Cédex 03, France

[b] National Institute of Materials Physics, Lab. Optics and Spectroscopy, Bucharest, P.O.Box MG-7, R-76900, Romania

Available online: 12 Jan 2012

To cite this article: S. Lefrant, J. P. Buisson, J. Y. Mevellec, F. Massuyeau, J. Wery, M. Baibarac & I. Baltog (2012): Anti-Stokes Raman Scattering and Luminescence in Carbon Nanotube Nanostructures, Molecular Crystals and Liquid Crystals, 554:1, 111-118

To link to this article: http://dx.doi.org/10.1080/15421406.2012.633816

Mol. Cryst. Liq. Cryst., Vol. 554: pp. 111–118, 2012

ISSN: 1542-1406 print/1563-5287 online
DOI: 10.1080/15421406.2012.633816

Taylor & Francis
Taylor & Francis Group

Anti-Stokes Raman Scattering and Luminescence in Carbon Nanotube Nanostructures

S. LEFRANT,[1,*] J. P. BUISSON,[1] J. Y. MEVELLEC,[1]
F. MASSUYEAU,[1] J. WERY,[1] M. BAIBARAC,[2]
AND I. BALTOG[2]

[1]Institut des Matériaux Jean Rouxel, 2 rue de la Houssinière, B.P.32229, 44322 Nantes Cédex 03 France
[2]National Institute of Materials Physics, Lab. Optics and Spectroscopy, Bucharest, P.O.Box MG-7, R-76900, Romania

In this paper, we present recent results obtained on single-walled carbon nanotubes (SWNTs) and carbon nanotube/conjugated polymer composites by using resonant Raman scattering and Surface Enhanced Raman Scattering (SERS). Besides the characterization of these materials, we report on peculiar properties observed in the anti-Stokes Raman branch of the Raman spectra. They consist in an abnormal anti-Stokes Raman emission which is explained by a mechanism reminiscent of a Coherent anti-Stokes Raman Scattering (CARS) emission. It results from a wave mixing process between the incident laser light and Stokes Raman light, generated by the SERS mechanism. In a parallel way, we have investigated in details the resonance effects which also induce anomalies in the anti-Stokes/Stokes intensity ratios, as a function of several parameters including the observation temperature, the environmental conditions, the dilution in solvents, etc. Studies extended to composites based on carbon nanotubes and conjugated polymers reveal also interesting properties. In the case of poly(bithiophene) (PBTh), one observes a strong amplification of the 1450 cm^{-1} Raman line in the anti-Stokes branch, generated by the plasmon excitation of metallic tubes. This phenomenon occurs in several other conjugated polymers such as PEDOT and PPV for modes located around 1500 cm^{-1}. The role of metallic SWNTs is discussed.

Finally, an anti-Stokes luminescence excited in the low energy tail of the absorption band of PPV and PPV/SWNTs composites has even been observed for the first time, explained through a phonon-energy up-conversion mechanism.

Keywords Carbon nanotubes; CARS emission; hybrid carbon nanotube/conjugated polymer materials; Raman scattering

1. Introduction

Carbon nanotubes, even if they have been extensively studied for two decades [1,2], are still attractive materials in their multiple forms, i.e. single walled carbon nanotubes (SWNTs), double walled carbon nanotubes (DWNTs), multi-walled carbon nanotubes (MWNTs) or even composites with either saturated or conjugated polymers. This is mainly due to their

*Address correspondence to Prof. S. Lefrant, Institut des Matériaux Jean Rouxel, 2 rue de la Houssinière, B.P.32229, 44322 Nantes Cédex 03 France. Tel.: +33 240 373 910; Fax: +33 240 373 995; E-mail: Serge.Lefrant@cnrs-imn.fr

unique properties, mechanical and/or electronic. As a consequence, efforts have been made for their use in electronic devices by various chemical treatments, in particular to achieve their functionalization as a way to focus on specific applications [3,4]. Carbon nanotubes have also been incorporated in different matrices to form composites and among them, those prepared with conjugated polymers. Beyond the goal of finding specific applications, fundamental phenomena have also recently emerged, as a consequence of using nanostructures such as those employed in Surface Enhanced Raman Scattering (SERS). SERS [5,6] has been used as complementary to resonant Raman scattering which permits the identification of metallic or semiconducting tubes by choosing an ad'hoc excitation wavelength, but also an evaluation of the tube diameter distribution [7,8]. The new phenomenon discovered by studying SERS spectra of carbon nanotubes or carbon nanotube/conjugated polymer composites consists in an abnormal emission in the anti-Stokes branch of Raman spectra, attributed to a Coherent anti-Stokes Raman Scattering (CARS) mechanism [9]. This result turns out to be significantly important in particular in composites when Raman scattering spectra are hidden by luminescence emission.

2. Results and Discussion

As mentioned several times in literature, Raman scattering has been widely used as a probe to characterized single walled carbon nanotubes [7,8]. In the 1400–1700 cm^{-1} range, the shape of the so-called G band has been shown to be of extremely important to identify semi-conducting or metallic tubes. It originates from the E_{2g2} mode of graphite and split in G^- and G^+ components in carbon nanotubes because of the curvature. These features are well defined and characteristics of semi-conducting tubes, whereas broader components are the signature of metallic tubes. In addition in this latter case, the G^- band is strongly asymmetric. Interpreted for a long time as due to an electron-plasmon coupling [11], more recent calculations have definitely proven that this phenomenon is accounted for by an electron-phonon coupling [12]. It remains that both semi-conducting and metallic tubes can be observed independently by a judicious choice of the excitation wavelength if one refers to the so-called Kataura plot [13] which correlates the tube diameter with the optical transition energies. In the low range of frequencies, one observes the radial breathing modes (RBMs) for which a direct relationship between frequencies and diameters allows to evaluate the tube diameter distribution, although several laws [14–19] can be found in literature and therefore, a great care has to be taken to account for the environment which plays a rather important role on the RBM frequencies. Finally, the D band, present in Raman spectra of all carbonaceous compounds, is characteristic of defects and disorder in carbon structures [20,21].

CARS-type phenomena were discovered some years ago as a way to interpret anomalies observed in the anti-Stokes spectrum of SWCNTs. Two kinds of anomalies were reported. The first one is due to resonance effects that induce asymmetry in Stokes and anti-Stokes band profiles, as interpreted by Brown et al [11]. The second anomaly was the quadratic behaviour observed in the anti-Stokes emission intensity when a SERS support was used. This was shown to occur in several materials such as cresyl violet, rhodamine G and carbon nanotubes [22]. K. Kneipp and co-workers [22] attributed this phenomenon to a consequence of an over-population of high vibrational states produced by the large phonon density of the excitation light. Some years later, it was demonstrated that a wave mixing process between the incident light and the Stokes Raman light can be generated by the SERS mechanism, yielding a CARS process. Notice that, in this type of experiments, using tightly focused beams, the phase matching rules turn out to be relaxed by the nanostructure itself [9,10].

In our studies of single walled carbon nanotubes, we have checked all parameters which have an effect on the intensity of the anti-Stokes Raman scattering. In regular CARS experiments, the anti-Stokes intensity can be described by the following equation:

$$I_{CARS} \propto N_A\, \omega_{as}^2 d^2 |\chi^{(3)}|^2\, I_l^2 I_s\, \sin c^2(|\Delta k|.d/2) \quad (1)$$

in which $\chi^{(3)}$ is the third order nonlinear dielectric susceptibility, d is the sample slab thickness, sinc(x) means sin(x)/x and N_A is the numerical aperture of the collecting lens.

The phase-matching condition $|\Delta k|\cdot d \ll \pi$ where $\Delta k = k_{as} - (2\, k_p - k_s)$ and k_{as}, k_s and k_p are the wave vectors of the anti-Stokes, Stokes and pump light, respectively, is fulfilled by the coherent nature of the CARS process itself. Indeed, for condensed media, if the beams cross at an angle θ, the small dispersion of refractive index makes $\Delta k \approx 0$ over small paths. Then, for tightly focused beams, the requirement of phase matching relaxes, being no longer sensitive to the Raman shift and so, a CARS spectrum can be observed at an angle θ_{as} larger than the Stokes angle θ_s. Therefore, the challenge is to demonstrate that at resonant laser excitations, when the excitation light coincides with an electronically allowed transition ($\chi^{(3)} \neq 0$), the intensity of the anti-Stokes emission is enhanced according to eq. (1). Then in the first stage of our studies, we focused our attention to check carefully how the most relevant parameters influence the anti-Stokes intensity. First of all, the use of a SERS substrate, i.e. a rough metallic surface of Au, Ag or Cu, was found to be necessary to induce CARS-type phenomena. Other parameters were investigated one by one, such as the $\chi^{(3)}$ influence, the numerical aperture of the microscope used to record Raman spectra, the intensity of the exciting laser light, the thickness of the sample and last but not least, the value of the anti-Stokes frequency, ω_{as}. All details can be found in Refs. [9,21].

Another important point deserves discussion, i.e. the role of the resonance effects. As already mentioned, anomalies in the anti-Stokes intensities have also been invoked, in particular for the RBM peaks. As an example, Fig. 1 reports the Stokes and anti-Stokes

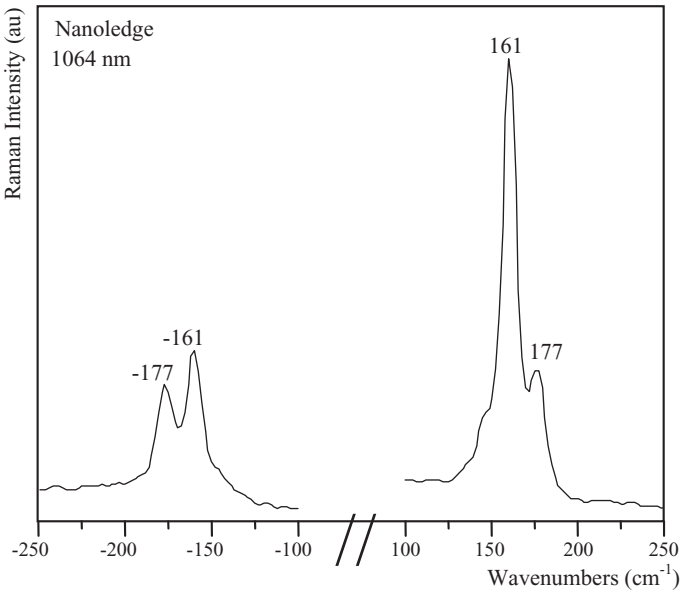

Figure 1. Stokes and anti-Stokes RBMs at 161 cm^{-1} and 177 cm^{-1} for arc discharge carbon nanotubes in powder form recorded with the 1064 nm excitation line (from ref. 23).

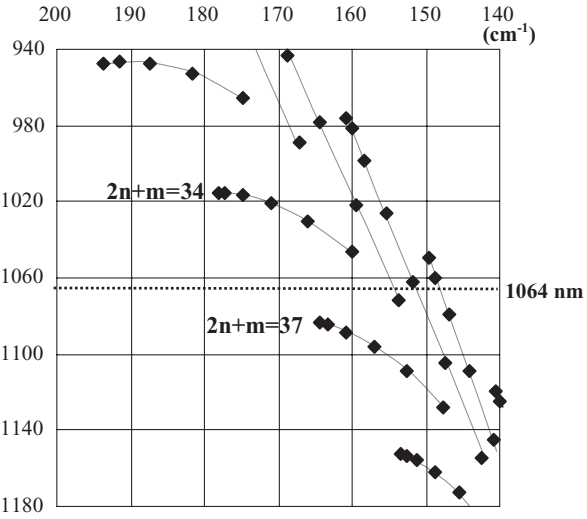

Figure 2. Part of the Kataura plot showing the tube families involved in the 1064 nm excitation energy.

RBM bands in the case of arc discharge tubes in powder. They consist of mainly two components at 161 and 177 cm^{-1} when one uses the $\lambda_{exc.} = 1064$ nm laser excitation. The Anti-Stokes/stokes ratios are measured to be 0.34 and 1.04 respectively. Previous experiments could make us think [22] that the mode at 161 cm^{-1} could be associated to isolated tubes whereas the one at 177 cm^{-1} to bundled tubes. Therefore one might use this phenomenon to identify isolated tubes from bundles [23]. In fact, as shown later, the differences in I_{AS}/I_S ratios do not arise from CARS but from resonance effects [24]. These effects are very sharp in SWNTs and depend on several parameters which make difficult a clear analysis. In Fig. 2, we have reported a partial part of the Kataura plot in the energy region associated with the 1064 nm excitation energy. Contrarily to the very first assignment we made for the 161 and 177 cm^{-1} peaks [23], many different tubes from different $2n + m$ families contribute to the RBM modes, those whose transition energy is close to the excitation one. They are consigned in Table 1. In the case described here, i.e. for the 1064 nm excitation, one catches, among others, the resonance with the tubes of the $2n + m = 37$ and 34 families, respectively. Notice that the 161 cm^{-1} band, which includes RB modes of the $2n + m = 37$ family is more intense than that of the $2n + m = 34$ one, the excitation energy being closer to the electronic transition. This interpretation explains also why any change in resonance conditions, due to interactions with the environment, will affect the relative intensity of these two bands. Similar studies were carried out on functionalized arc discharge tubes and a systematic analysis in the range of excitations between 700 and 750 nm yielded a clear determination in the maximum electronic transitions as a function of the chemical groups attached to the tubes. Details are published elsewhere [25].

To summarize this part of the work, the anomalous intensity ratios between modes in the anti-Stokes and Stokes branches of the Raman spectra have a twofold origin. On one hand, at low frequency, this is due to resonance effects which are strongly dependent upon several parameters such as temperature, state of aggregation, functionalization of the tubes as well as their charge state. At higher frequencies ($\sim$1500 cm^{-1}), the high intensity in

Table 1. RBM Frequencies of SWNTs according to their 2n + m family and Hamada indexes n and m. Values of frequencies in bold characters are the expected most intense modes

2n + m	(n, m)	Frequency (cm^{-1})	2n + m	(n, m)	Frequency (cm^{-1})
34	(17,0)	178	37	(18,1)	**165**
	(16,2)	177		(17,3)	**163**
	(15,4)	175		(16,5)	**161**
	(14,6)	171		(15,7)	**157**
	(13,8)	166		(14,9)	153
	(12,10)	**160**		(13,11)	148
35	(12,11)	154	38	(15,8)	152
41	(20,1)	150			
	(19,3)	149			
	(18,5)	147			

the anti-Stokes branch comes from a CARS-type effect induced through the SERS surface nanostructures and can be observed in different systems as discussed below.

As a matter of fact, a similar observation can be made in several other structures. It has already been shown that modes around 1500 cm^{-1} can be intense in the case of poly-bithiophene deposited on SERS substrates [26]. Also in poly(3,4-ethylendioxythiophene) (PEDOT), the role of the resonance conditions for inducing such an effect has been put in evidence by changing the laser excitation wavelength from 514.5 nm to 676.4 nm. Details have been published in Ref. 27 and these results corroborate the fact that the coefficient $\chi^{(3}$ has to be non-zero in such a mechanism. We have also investigated composites made of SWNTs and poly-phenylene vinylene (PPV), known as a very efficient luminescent polymer. This polymer has been extensively studied for almost three decades as a potential candidate for being used in light emitting diodes. Several derivatives of this polymer have also been investigated to improve in particular their processability in thin films. In our case, we have re-visited the interpretation of the luminescence properties and introduced the concept of the bimodal distribution of chain lengths [28]. We demonstrated its importance to explain luminescence data as a function of temperature, but also in the case of composites with SWNTs. One observes in this later case a drastic reduction of the chain conjugation length and the relative intensity of the luminescence bands is strongly affected. Concerning the CARS effect in these composites, an amplification of the anti-Stokes spectrum of PPV is observed (Ref. 24), but the content of SWNTs in the composite is also an important factor. Figures 3a and b show two examples of SWNT/PPV composites with mass concentrations of SWNTs of 16 and 32% respectively. In Fig. 2b, one observes in the Stokes spectrum the well-known features of PPV, which are also present in the anti-Stokes branch in larger intensity than expected by the Maxwell-Boltzman law (red curve in the spectrum). The amplification has been calculated to be 17 and 7 for the bands at 1583 and 1170 cm^{-1}, respectively. Notice that, due to their low concentration in the composite, SWNTs are not clearly visible in this spectrum. In Fig. 3b, we show the Raman spectrum, under similar conditions, of a composite sample containing 32% of SWNTs. In this case, a weak SWNT Raman spectrum is superimposed to that of PPV. The important feature to put forwards in this case is the PPV spectrum in the anti-Stokes branch, for which the amplification ratios for the same 1583 and 1170 cm^{-1} bands are now 36 and 12.7,

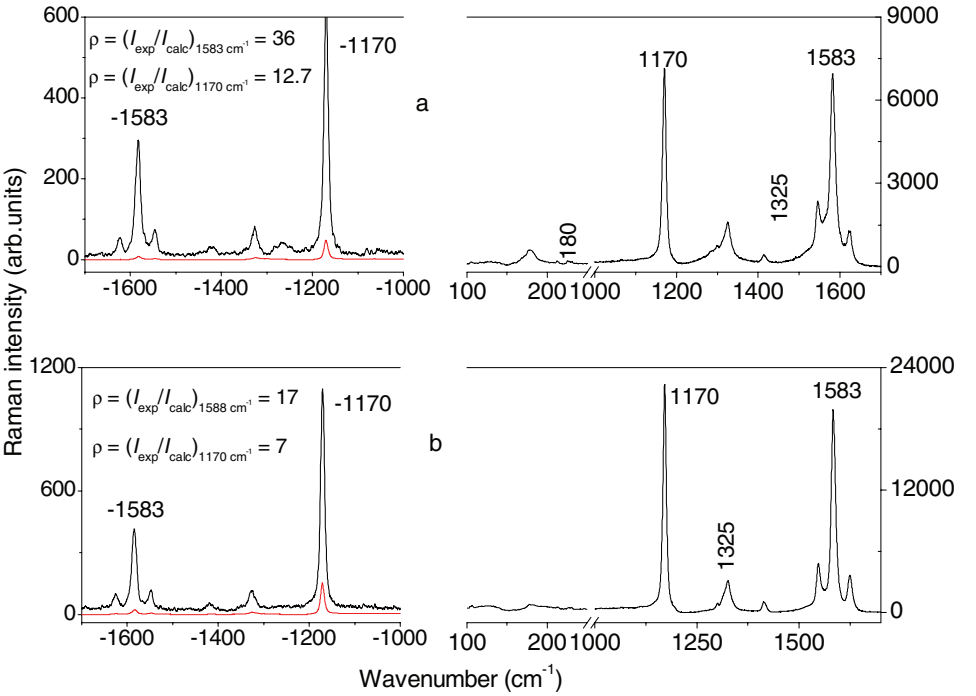

Figure 3. Anti-Stokes and Stokes Raman spectra of SWNT/PPV composites deposited on an Au substrate with an excitation of 676.4 nm. The red curve shows the anti-Stokes replica calculated with the Boltzmann formulae applied to the measured Stokes Raman spectrum. a): SWNT mass concentration 32%, b) SWNT mass concentration 16%.

respectively, increased by a factor of two as compared to the previous case. This important result can be seen in the following way. First, the SERS substrate itself induces a CARS-type phenomenon as demonstrated initially. Second, the presence of nanotubes in a polymer matrix induces a further amplification of the polymer vibrational modes. This amplification is dependent on the nanotube concentration. We expect metallic tubes to be responsible for this phenomenon, although further experiments would be needed, such as those conducted with only one category of tubes, either metallic or semi-conducting. More recently, we have put in evidence in the same PPV/SWNT composites a luminescence in the anti-Stokes region, i.e. at higher energy than excitation. The effect is explained through a phonon-energy up-conversion mechanism that is improved by the increase of the carbon nanotube contents in PPV/SWNTs composites. The up-conversion process is argued by the enhancement of the emission band at 2.39 eV with the increase of the excitation light intensity.

4. Conclusions

In this paper, we have briefly described the origin of anomalous anti-Stokes Raman intensities observed in nanostructures such as single-walled carbon nanotubes (SWNTs) deposited on rough metallic surfaces used as SERS substrates. We have identified two different effects, one consists in a CARS-type phenomenon which induves a strong amplification in the high frequency range. The other phenomenon is described by resonance effects which

yield anti-Stokes/Stokes ratios which do not follow the usual Maxwell-Boltzmann law, particularly in the low frequency range wher RBMs are observed.

In composite materials made with SWNTs and conjugated polymers, similar amplifications of the polymer vibrational modes are observed. We demonstrate in addition that the SWNT content plays a significant role in this amplification. We expect metallic tubes to be responsible of these effects, although further experiments are undoubtedly needed to elucidate this point.

Acknowledgments

This work was performed in the frame of the Scientific Cooperation between the the Institute of Materials Jean Rouxel in Nantes, and the Laboratory of Optics and Spectroscopy of the National Institute of Materials Physics, Bucharest. A part of this work was supported by the Romania Research Projects PN II 62081 and PN II 72182.

References

[1] Iijima, S. (1991). *Nature*, *354*, 56.
[2] Tomanek, D., Jorio, A., Dresselhaus, M. S., & Dresselhaus, G. (2008). *Topics in Applied Physics*, *111*, 1.
[3] Banerjee, S., Hemraj-Benny, T., & Wong, S. S. (2005). *Adv. Mat.*, *17*, 17.
[4] Hirsch, A. (2002). *Angew. Chem. Int. Ed.*, *41*, 1853.
[5] Lefrant, S., Baltog, I., Lamy de la Chapelle, M., Baibarac, M., Louarn, G., Journet, C., & Bernier, P. (1999). *Synth. Met.*, *100*, 13.
[6] Kneipp, K., Wang, Y., Kneipp, H., Itzkan, I., Dasari, R. R., & Feld, M. S. (1996). *Phys. Rev. Lett.*, *76*, 244.
[7] Dresselhaus, M. S., Dresselhaus, G., Jorio, A., Souza Filho, A. G., & Saito, R. (2002). *Carbon 42*, 2043 and references therein.
[8] Dresselhaus, M. S., Dresselhaus, G., Saito, R., & Jorio, A. (2005). *Physics Reports 409*, 47 and references therein.
[9] Baltog, I., Baibarac, M., & Lefrant, S. (2005). *Phys. Rev. B*, *72*, 245402.
[10] Baltog, I., Baibarac, M., & Lefrant, S. (2008). *Physica E*, *40*, 2380.
[11] Brown, S. D. M., Jorio, A., Corio, P., Dresselhaus, M. S., Dresselhaus, G., Saito, R., & Kneipp, K. (2001). *Phys. Rev. B*, *63*, 155414.
[12] Piscanec, S., Lazzeri, M., Robertson, J., Ferrari, A. C., & Mauri, F. (2007). *Phys. Rev. B*, *75*, 035427.
[13] Kataura, H., Kumazawa, Y., Maniwa, Y., Umczu, I., Suzuki, S., Ohtsuka, Y., & Achiba, Y. (1999). *Synth. Met.*, *103*, 2555.
[14] Jorio, A., Saito, R., Hafner, J. H., Lieber, C. M., Hunter, M., McClure, T., Dresselhaus, G., & Dresselhaus, M. S. (2001). *Phys. Rev. Lett.*, *86*, 1118.
[15] Bachilo, S. M., Strano, M. S., Kittrell, C., Hauge, R. H., Smalley, R. E., & Weissman, R. B. (2002). *Science*, *298*, 2361.
[16] Kurti, J., Gresse, G., & Kuzmany, H. (1998). *Phys. Rev. B*, *58*, R8869.
[17] Kramberger, C., Pfeiffer, R., Kuzmany, H., Zolyomi, V., & Kurti, J. (2003). *Phys. Rev. B*, *68*, 235404.
[18] Meyer, J. C., Paillet, M., Michel, T., Moréac, A., Neumann, A., Duesberg, G., Roth, S., & Sauvajol, J. L. (2005). *Phys. Rev. Lett.*, *95*, 217401.
[19] Tuinstra, F., & Koenig, J. L. (1970). *J. Chem. Phys.*, *53*, 1126.
[20] Thomsen, C., & Reich, S. (2000). *Phys. Rev. Lett.*, *85*, 5214.
[21] Baltog, I., Baibarac, M., & Lefrant, M. (2005). *J. Opt. A: Pure Appl. Opt.*, *7*, 1.
[22] Marcoux, P. R., Schreiber, J., Batail, P., Lefrant, S., Renouard, J., Jacob, G., Albertini, D., & Mevellec, J. Y. (2002). *Phys. Chem. Chem.Phys.*, *4*, 2278.

[23] Lefrant, S., Buisson, J. P., Mevellec, J. Y., Baibarac, M., & Baltog, I. (2008). *Phys. Status Solidi (b)*, *245*, 2221.
[24] Lefrant, S., Buisson, J. P., Mevellec, J. Y., Baibarac, M., & Baltog, I. (2011). *Opt. Mat.*, *33*, 1410.
[25] Mevellec, J. Y., Bergeret, C., Cousseau, J., Buisson, J. P., Ewels, C., & Lefrant, S. (2011). *J. Am. Chem. Soc.*, *133*, 16938.
[26] Baibarac, M., Baltog, I., & Lefrant, S. (2009). *Carbon 47*, n° 5, 1389.
[27] Baltog, I., Baibarac, M., Lefrant, S., & Mevellec, J. Y. (2010). *J. Raman spectrosc.*, *42*, 303.
[28] Mulazzi, E., Ripamonti, A., Wery, J., Dulieu, B., & Lefrant, S. (1999). *Phys. Rev. B*, *60*, 16519.